

Oscillations of the Horizontal Intrusion in a Side-Heated Cavity

F. Xu, J.C. Patterson and C. Lei

School of Engineering, James Cook University, QLD 4811, AUSTRALIA

Abstract

In this study, a two dimensional numerical simulation of natural convection in a side-heated cavity is carried out. The evolution of the hot horizontal intrusion is observed and its physical properties are described. The results show that after the hot intrusion reaches the cold wall, due to the hot fluid accumulation and the associated buoyancy effect in the cold top corner, a flow opposing the cold boundary layer flow firstly appears and then forms a local circulation. This circulation then moves back to the hot wall, and eventually a cavity-scale oscillation is formed between the hot and cold walls underneath the ceiling of the cavity.

Introduction

Natural convection in a rectangular side-heated cavity is a problem of fundamental interest to fluid mechanics, with many industrial applications such as electronic cooling systems, heat exchangers, solar water heaters and crystal growth procedures. Studies of this topic have been conducted for many years since Batchelor [1] first presented natural convection in a cavity of a large aspect ratio with a temperature difference between the sidewalls. Based on a detailed scaling analysis, Patterson & Imberger [2] portrayed the physical processes and features of the natural convection caused by abruptly heating and cooling two sidewalls respectively, and classified the laminar transient flow from the start-up to the steady state into different flow regimes. Major flow regimes include the vertical boundary layer growth, the horizontal intrusion and approach to steady state, which have been validated by experimental measurements [3] and numerical simulations [4]. Accompanying the above-mentioned theoretical analyses [1, 2], many significant experimental and computational results have been subsequently obtained in the context of the basic flow in a side-heated cavity. A representative experiment by Ivey [3] firstly and rather comprehensively described certain kinematic properties of the transient flow. The basic flow field was visualized in [3], and separation of the horizontal intrusion from the horizontal boundary was observed. Another comprehensive numerical and experimental description of the flow evolution in a side-heated cavity was reported in [5], and some basic physical properties of the transient flow were discussed.

It is known that a vertical boundary layer flow firstly appears when the sidewall of a cavity is abruptly heated or cooled. A distinct feature of the transient boundary layer flow is the leading-edge effect (LEE), which is characterised by high-frequency oscillations and even turbulence of natural convection in the side-heated cavity [6, 7]. A major discrepancy between the theoretical predictions and experimental measurements of the arrival time of the LEE was resolved by Armfield & Patterson [6] and Patterson et al [7] who confirmed that the arrival time of the LEE was determined by the velocity of the travelling waves which comprised the LEE. Another important feature of the vertical boundary layer is entrainment, which was discussed by Wright & Gebhart [8]. It is expected that the entrainment play a

key role in the transition of the vertical boundary layer from the start-up to quasi-steady state.

The horizontal intrusion is another important physical process in the side-heated cavity. The flow structure of the horizontal intrusion was visualized using the shadowgraph technique [9]. Contradictory explanations have been given in the literature for the mechanism responsible for the separation of the transient intrusion. Ivey [3] suggested that an internal hydraulic jump resulted in the separation. This explanation was supported by Paolucci & Chenoweth [4], but questioned by Patterson & Armfield [5] and Ravi et al [10]. It was suggested in [10] that the separation resulted from thermal effects; that is, the relatively cold fluid detached from the ceiling under the action of buoyancy forces when it reached the hot top corner. However, this explanation is not convincing because the fluid in the cavity core is not stratified in the early intrusion stage, and thus there is no 'colder' part of the intrusion relative to the ambient fluid near the hot top corner. The authors are currently investigating the dynamic mechanisms that are responsible for the separation of the horizontal intrusion flow, and the outcomes will be reported separately.

Despite of a large body of literature devoted to the transient natural convection boundary layer flow in a side-heated cavity over the last two decades, limited attention has been paid to the evolution of the horizontal intrusion after the start-up, which will be the primary focus of the present investigation.

Numerical procedures

Under consideration is a two-dimensional rectangular domain. The dimensions of the physical domain are based on the experimental model described in [11], that is, 0.24-m high (H) by 1-m long (L). The working fluid is water. The two-dimensional Navier-Stokes and energy equations with Boussinesq approximation to be solved are as follows

$$u_x + v_y = 0, \quad (1)$$

$$u_t + uu_x + vv_y = -\rho^{-1}p_x + \nu(u_{xx} + v_{yy}), \quad (2)$$

$$v_t + uv_x + vv_y = -\rho^{-1}p_y + \nu(v_{xx} + v_{yy}) + g\beta(T - T_m), \quad (3)$$

$$T_t + uT_x + vT_y = \kappa(T_{xx} + T_{yy}), \quad (4)$$

where T is the temperature, p pressure, u the velocity in the x -direction, v the velocity in the y -direction, g the acceleration due to gravity, β the coefficient of thermal expansion, κ the thermal diffusivity, and ν the kinematic viscosity. Subscripts represent partial differentiation except that T_m denotes a mean temperature. The SI units are adopted for all quantities throughout the paper.

The boundary conditions are shown in figure 1 along with the coordinate system, with the origin located at the center of the cavity. Initially, the fluid in the cavity is motionless and isothermal.

The above equations are solved using the SIMPLE scheme, where the spatial derivatives are discretized with a second-order upwind scheme. In order to accurately capture the features of the boundary layer flows, a non-uniform grid system is constructed with finer grids in the vicinity of wall boundaries. A $165 (H) \times$

463 (L) mesh is adopted with the smallest cells of $0.2 \times 0.2 \text{ mm}^2$ at the corners and a mesh expansion factor of 1.04 along both the horizontal and vertical directions toward the center of the domain (a similar mesh system was used in [5]). In addition, a finer mesh (199×563) and a coarser mesh (133×387) are also tested. The results of the mesh dependence test are shown in figure 2, which plots the time series of the calculated temperature at a point within the hot boundary layer for each mesh. Clearly, the two finer meshes produce almost identical results, and thus the medium fine mesh (165×463) is eventually adopted. Time marching is done by a second order implicit scheme. It is found that a time step of 0.4 second (smaller than that used in [5]) is sufficiently small to capture the features of the intrusion, and the stability of the scheme is also guaranteed for the non-uniform grids.

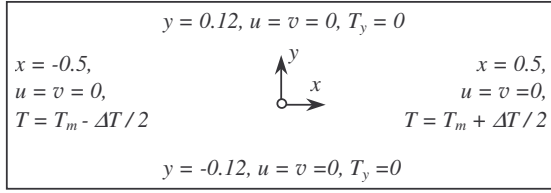


Figure 1: Physical domain and boundary conditions.

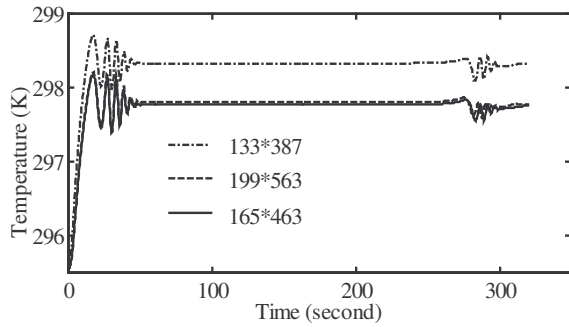


Figure 2: Time series of the temperature at ($x = 0.498$, $y = 0.09$) obtained with different meshes.

In the present investigation, the temperature difference between the two sidewalls is fixed at 16 K and the mean temperature is 295.55 K. The corresponding Rayleigh number and Prandtl number, which are defined below, are 3.77×10^9 and 6.64, respectively,

$$Ra = \frac{g\beta\Delta TH^3}{\nu\kappa}, \quad (5)$$

$$Pr = \frac{\nu}{\kappa}. \quad (6)$$

Results and Discussions

The present study focuses on the horizontal intrusion. Since the intrusion flow impacts on other flows within the core and the boundary layers, naturally, some kinematic properties of other flows in the side-heated cavity are also described.

Figure 3 shows plots of the temperature contours and stream functions at different times of the early stage of the flow development. In all the figures, the hot wall is to the right. It is seen in figure 3(a) that a group of trailing waves of the hot intrusion appear in the upper-right corner. In the meantime, a large anticlockwise circulation (hereinafter referred to as the *front circulation*) under the intrusion front is generated by a strong shear as seen in 3(b). With the passage of time, those trailing waves gradually regress to the hot top corner as shown in

3(c), and the *front circulation* arrives at the cold sidewall in 3(d). The *front circulation* then moves downstream along the cold sidewall in 3(f) and eventually dissipates into the core 3(h). Since the cold sidewall cannot cool and entrain all the hot intrusion to the bottom, increasing hot fluid is accumulated in the cold top corner (the upper-left corner). As a consequence, a tilted flow field forms near the cold top corner as shown in 3(h). In addition, the intrusion front stretches gradually downward along the cold sidewall, as indicated by the temperature contours shown in 3(e) and 3(g).

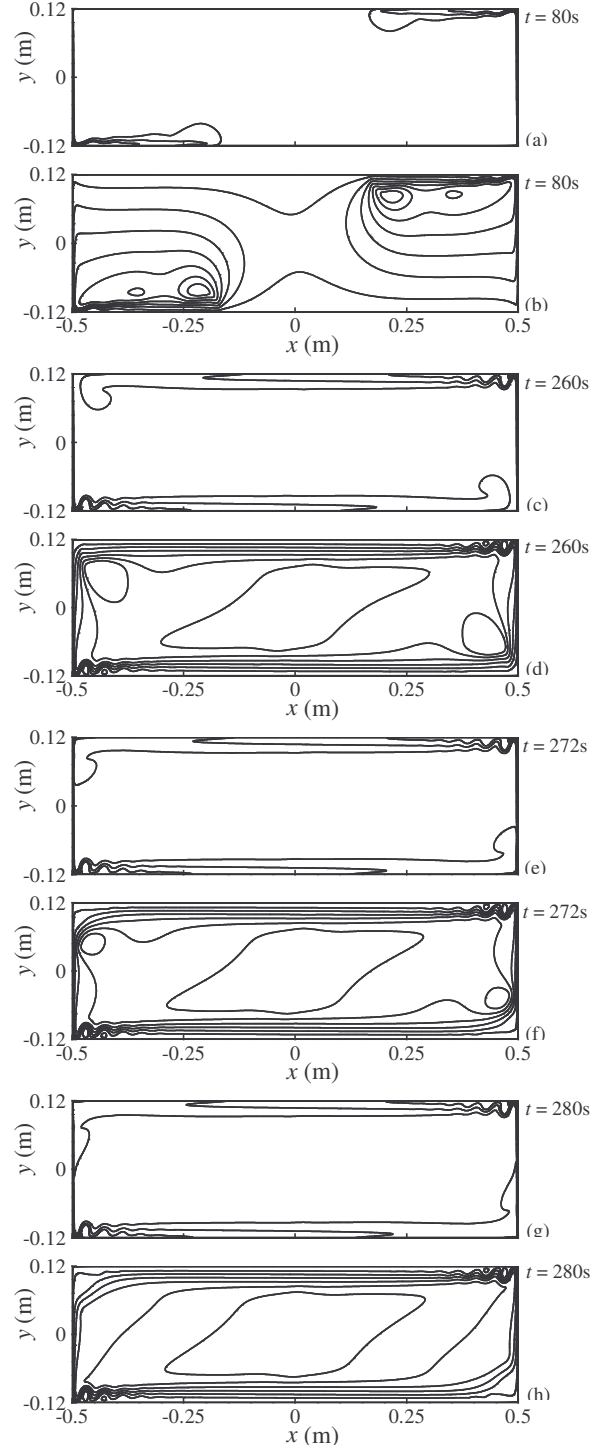


Figure 3: (a), (c), (e) and (g) temperature contours. (b), (d), (f) and (h) streamlines.

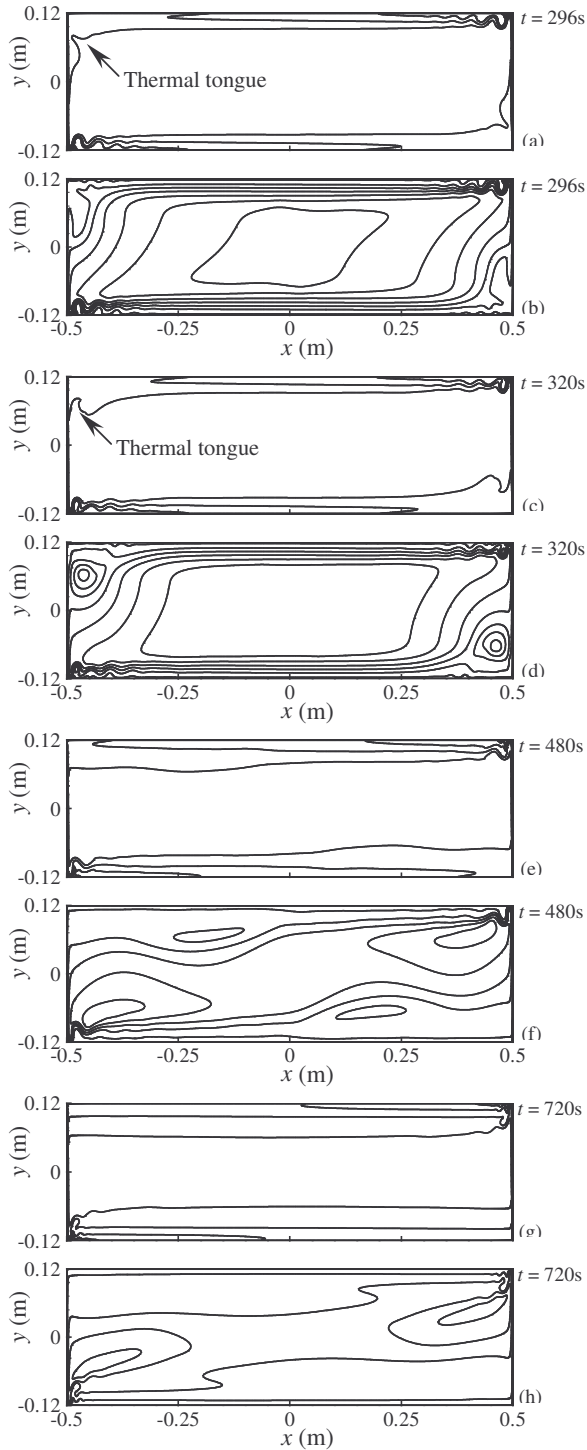


Figure 4: (a), (c), (e) and (g) temperature contours. (b), (d), (f) and (h) streamlines.

Likewise, a tilted density field is also generated near the cold top corner as can be seen in figure 3(g), and some buoyancy forces are associated with the tilted density field.

The subsequent flow development is shown in figure 4. As a consequence of the above-mentioned buoyancy effect, a reverse flow near the cold sidewall is generated as shown in 4(b). At this time, the temperature contours exhibit an upward 'thermal tongue' near the upper corner of the cold sidewall in 4(a). As the

hot intrusion further accumulates in the cold top corner, the increasing buoyancy effect forces the thermal 'tongue' to rotate in the clockwise direction 4(c), and eventually, a clockwise circulation as shown in 4(d) is formed in the region.

Figure 4(f) shows that this clockwise circulation is travelling toward the hot sidewall, although it has been weakened significantly. Moreover, the clockwise circulation splits the hot intrusion into two parts, one of which continues to run to the cold sidewall along the ceiling and the other jets into the core as seen in 4(f). After about 720 seconds, the clockwise circulation is completely dissipated and forms a reverse flow relative to the hot intrusion as shown in 4(h). This reverse flow then pushes the trailing waves near the hot (upper-right) corner closer to the hot sidewall (4g). It also impacts on the flow properties and structure of the hot vertical boundary layer. In addition, it is clear in figure 4 that the temperature contours in the upper part of the cavity move downward toward the core as the reverse flow moves back to the hot sidewall. This implies that the reverse flow speeds up the core stratification.

For the purpose of gaining insights into the details of the flow near the cold top corner when the hot intrusion reaches the cold wall, figure 5 shows the velocity vector field at the same time as of figure 4(d). It is seen in this figure that the strong shear between the clockwise circulation and the hot intrusion underneath the ceiling induces some smaller scale circulations in the region as well as some waves in the coming hot intrusion. A detailed discussion on the corresponding kinematic and dynamic mechanisms as well as the evolution of these waves will be reported separately.

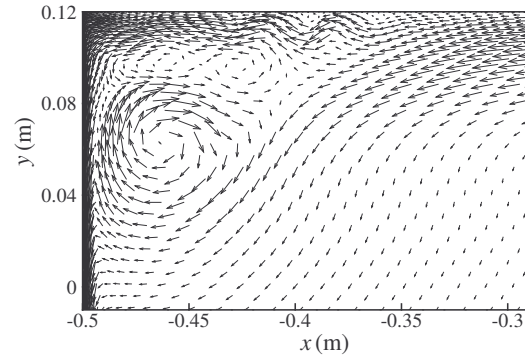


Figure 5: Velocity field in the cold top corner at 320s.

As shown in figure 4(h), the reverse flow has been significantly dissipated when it moves toward the hot sidewall. However, this flow does not disappear, and eventually it causes a cavity-scale oscillation in the upper part of the cavity (a back and forth flow between the hot and cold walls). Figure 6(a) shows this cavity-scale horizontal oscillation using a time series of the horizontal velocity obtained at the point $(x = 0, y = 0.07)$. It is seen that the amplitude of the oscillations decreases significantly after the first oscillation cycle as indicated by I in figure 6(a). The first two cycles (I and II in figure 6a) are completed by 1400 seconds, but the oscillation actually lasts for a longer time with reduced amplitude. At the point shown, the time duration for which the velocity is positive (the reverse flow) is more than 200 seconds. Despite of the reduced intensity of the cavity-scale oscillation, it plays a key role in the stratification of the core, as shown in figure 4.

Similarly, there always exists a symmetrical oscillation of the cold intrusion in the lower part of the cavity. Figure 6(b) shows the horizontal velocity profile at $x = 0$ at different times. Two symmetrical oscillations, one in the upper part and the other in

lower part of the cavity respectively, can be clearly observed in figure 6(b).

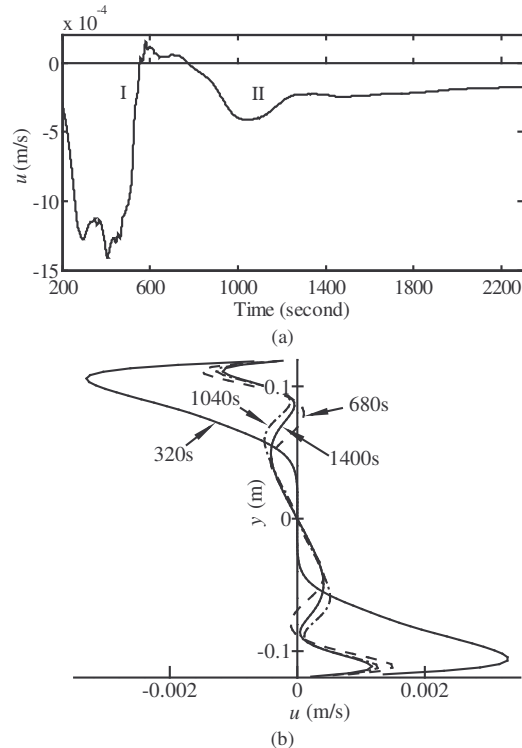


Figure 6: (a) Horizontal velocity (u) against time at the point ($x = 0, y = 0.07$). (b) Horizontal velocity profile at $x=0$ at 320, 680, 1040 and 1400s.

Conclusions

This paper focuses on the horizontal intrusion generated in the suddenly heated and cooled cavity. The physical properties of the intrusion are described, and a back and forth flow between the hot and cold walls is observed.

The numerical results show that some trailing waves initially evolve from the intrusion and a large anticlockwise circulation below the hot intrusion front forms. With the passage of time, this anticlockwise circulation moves horizontally to the cold sidewall and eventually dissipates. Subsequently, another clockwise circulation, close to the cold sidewall, is generated. This clockwise circulation produces a strong shear with the hot intrusion underneath the ceiling, inducing some smaller scale circulations and waves in the hot intrusion. The clockwise circulation moves back to the hot sidewall and forms an oscillation (a back and forth flow between the hot and cold walls). The oscillation is typical of the internal gravity wave of natural convection in a side-heated cavity, and can impact on both the vertical boundary layer flow and stratification of the

fluid in the core to some extent. This is because, on one hand, the oscillation can push the trailing waves in the hot top corner closer to the hot wall, thus changing the properties and structure of the hot vertical boundary layer flow; on the other hand, the hot intrusion into the core is split by the back and forth flow and speeds up the core stratification.

In conclusion, oscillations of the horizontal intrusion can play a key role in the transition of natural convection in a side-heated cavity. A more detailed kinematic description and dynamic discussion related to this issue will be reported separately.

Acknowledgments

Useful discussions with Steve Armfield and Yong Sha and the financial support by the Australian Research Council are gratefully acknowledged.

References

- [1] Batchelor, G.K., Heat Transfer by Free Convection across a Closed Cavity between Vertical Boundaries at Different Temperatures, *Quart. Appl. Math.*, **12**, 1954, 209-233.
- [2] Patterson, J.C. & J. Imberger, Unsteady Natural Convection in a Rectangular Cavity, *J. Fluid Mech.*, **100**, 1980, 65-86.
- [3] Ivey, G.N., Experiments on Transient Natural Convection in a Cavity, *J. Fluid Mech.*, **144**, 1984, 389-401.
- [4] Paolucci, S. & D. R. Chenoweth, Transition to Chaos in a Differentially Heated Vertical Cavity, *J. Fluid Mech.*, **201**, 1989, 379-410.
- [5] Patterson, J.C. & S.W. Armfield, Transient Features of Natural Convection in a Cavity, *J. Fluid Mech.*, **219**, 1990, 469-497.
- [6] Armfield, S.W. & J.C. Patterson, Wave Properties of Natural-Convection Boundary Layers, *J. Fluid Mech.* **239**, 1992, 195-211.
- [7] Patterson, J.C., Graham, T., Schöpf, W. & S.W. Armfield, Boundary Layer Development on a Semi-Infinite Suddenly Heated Vertical Plate, *J. Fluid Mech.*, **453**, 2002, 39-55.
- [8] Wright, N.T. & B. Gebhart, The Entrainment Flow Adjacent to an Isothermal Vertical Surface, *Int. J. Heat and Mass Transfer*, **37**, 1994, 213-231.
- [9] Schöpf, W. & J.C. Patterson, Visualization of Natural Convection in a Side-Heated Cavity: Transition to the Final Steady State, *Int. J. Heat Mass Transfer*, **39**, 1996, 3497-3509.
- [10] Ravi, M.R., Henkes, R.A.W.M. & C.J. Hoogendoorn, On the High-Rayleigh-Number Structure of Steady Laminar Natural-Convection Flow in a Square Enclosure, *J. Fluid Mech.*, **262**, 1994, 325-351.
- [11] Brassington, G.B., Lee, M. & J.C. Patterson, Observations of a Transient Stratified Laminar Intrusion, in Proc. 7th Australian Heat and Mass Transfer Conference, editor G.B Brassington and J.C. Patterson, Chalkface Press, 2000, 45-51.